Desalination and Water Treatment
www.deswater.com

doi: 10.1080/19443994.2016.1174740

57 (2016) 27794–27803
December

Taylor & Francis
Taylor & Francis Group

Effect of operating parameters on trichloroethylene degradation by extended release of nanoscale zero-valent iron

Chiu-Wen Chen, Te-San Chen, Kuo-Feng Hsia, Chih-Feng Chen, Cheng-Di Dong*

Department of Marine Environmental Engineering, National Kaohsiung Marine University, Kaohsiung 81157, Taiwan,
Tel. +886 7 3617141, ext. 3761; Fax: +886 7 365 0548; email: cwchen@mail.nkmu.edu.tw (C.-W. Chen),
Tel. +886 7 3617141, ext. 3777; Fax: +886 7 365 0548; email: chents@mail.nkmu.edu.tw (T.-S. Chen),
Tel. +886 7 3617141, ext. 3765; Fax: +886 7 365 0548; email: e791122888@hotmail.com (K.-F. Hsia),
Tel. +886 7 3617141, ext. 3762; Fax: +886 7 365 0548; emails: dong3762@mail.nkmu.edu.tw (C.-F. Chen),
cddong@mail.nkmu.edu.tw (C.-D. Dong)

Received 5 October 2015; Accepted 30 March 2016

ABSTRACT

This study investigated the effects of various operating parameters on the efficiency and kinetics of trichloroethylene (TCE) degradation by commercial, polyvinyl alcohol-co-vinylacetate-co-itaconic acid (PV3A) stabilized nanoscale zero-valent iron (PV3A-nZVI). The results showed that TCE degradation was a pseudo-first-order reaction. The degradation efficiency and the apparent rate constant of TCE increased with the increasing PV3A-nZVI dosage and decreased with the increasing initial TCE concentration and pH. In addition, the effect of the solution matrix was evaluated. The results suggested that increasing the seawater ratio in the solution suppressed TCE degradation. The apparent rate constants of TCE decreased from 2.79×10^{-2} to 9.10×10^{-3} min^{-1}, and the seawater ratio increased from zero to 100% at 5 g/L PV3A-nZVI and 10 mg/L TCE. Moreover, an investigation of TCE degradation products confirmed that reductive dechlorination through the successive loss of chloride ions is the main pathway of TCE degradation, and ethene is the predominant byproduct during TCE dechlorination. Notably, nearly 100% TCE (10 g/L) removal was achieved with 5 g/L PV3A-nZVI in pure water and seawater within 90 and 120 min, respectively. Hence, PV3A-nZVI is a promising technology for remediating surface water, groundwater, and seawater matrices contaminated with TCE.

Keywords: Nanoscale zero-valent iron; Trichloroethylene; Degradation efficiency; Dechlorination

---

1. Introduction

Trichloroethylene (TCE), a chlorinated aliphatic hydrocarbon, is a colorless liquid with a sweet odor and is widely used in dry cleaning and as a metal degreaser, chemical intermediate, extractant, and electroplating [1]. TCE possess many harmful characteristics such as high carcinogenicity, toxicity, and flammability [2]. Hence, it is ranked number 16 of the 275 substances in the Priority List of Hazardous Substances of the Agency for Toxic Substances and Disease Registry and is listed as a priority pollutant in Taiwan.

The production volume of TCE was 146,000 tons in 1991 in the United States [3] and approximately

---

*Corresponding author.

1944-3994/1944-3986 © 2016 Balaban Desalination Publications. All rights reserved.

250,000 tons in 2011 in China, and its demand has increased gradually in recent years [4]. TCE is poorly soluble in water, and the main sources through which TCE is released in the environment are sewage effluents, leakage from storage tanks, and sometimes improper disposal practices. TCE is often found in soil, sediment, groundwater, and surface water. Recently, TCE-contaminated sites have been found worldwide. TCE has been detected in at least 60% of the US EPA's Superfund National Priorities List sites [1,5], and it is the most frequently reported organic compound in groundwater. In China, TCE is the most commonly detected contaminant in the environment [6,7]. Moreover, some sites have been heavily contaminated by TCE in Taiwan. For example, the RCA site in Taoyuan is contaminated by TCE and pentachloroethylene. TCE is not easily biodegraded by natural attenuation. In general, conventional sewage treatment plants cannot effectively remove TCE in wastewater. Therefore, the development of effective approaches for removing TCE to minimize its contamination in the environment is urgently required. Recently, studies have used the following methods for removing TCE: ozonation [8], photocatalytic degradation [9], Fenton oxidation [10], electrochemical dechlorination [11], and zero-valent reduction [12]. However, secondary pollutants may be formed during ozonation or Fenton oxidation. Although TCE can be rapidly degraded using photocatalytic and electrochemical processes, energy consumption may be high.

During the past decade, studies have shown nanoscale zero-valent iron (nZVI) particles to be a promising technology for remediating water contaminated with halogenated organic compounds, such as TCE [12,13], chloroethenes [14], and polychlorobiphenyls [15]. Chlorinated compounds can be effectively degraded to less harmful species through reductive dehalogenation by zero-valent ions. Furthermore, nZVI has various advantages such as wide application, simple equipment, easy operation, a low-temperature requirement, and no sludge formation. However, the application of nZVI technology still faces several challenges including a strong agglomeration tendency, rapid sedimentation, and consequently limited mobility of nanoparticles in the aquatic environment. Recently, various methods have been developed for modifying nZVI particles, enhancing their reactivity, improving their suspension stability, and prolonging the activity of nZVI [12,16–19]. Polyvinyl alcohol-co-vinyl acetate-co-itaconic acid (PV3A) was identified as the most promising material for achieving a stable suspension of the nZVI nanoparticles [16]. Moreover, Shih et al. [20] indicated that PV3A stabilization of nZVI nanoparticles enables maintaining a more reductive reaction system for long-term exposure in wastewater. Therefore, the use of PV3A-stabilized nZVI nanoparticles (PV3A-nZVI) for TCE degradation is an appealing approach.

The degradation efficiency and kinetics of TCE dechlorination by PV3A-nZVI vary according to several operating parameters, namely the PV3A-nZVI dosage, initial TCE concentration, solution pH, and sample matrices. To the best of our knowledge, few studies have been conducted on the performance of TCE degradation using PV3A-nZVI in a real seawater matrix. The interference of real seawater with TCE degradation has not been addressed clearly. Therefore, in this study, batch tests were conducted for investigating TCE degradation to evaluate the effect of operating parameters on the removal efficiency and degradation kinetics of TCE and to identify the reaction mechanism of TCE degradation. The obtained data support the use of PV3A-nZVI as a practical water treatment method for removing TCE.

2. Experimental

2.1. Chemicals

PV3A-nZVI particles (purity >99%, size <100 nM) were purchased from GeoNano Environmental Technology, Inc. (Taiwan). Before use, the particles were stored in an ethanol solution at 4°C in the dark to avoid the formation of iron oxide-hydroxide (i.e. FeOOH) on the fresh nZVI surface. Analytical-grade TCE (C_2HCl_3) was purchased from LABSCAN (Thailand). Sulfuric acid and sodium hydroxide were purchased from SHOWA (Japan). The deionized water used to prepare the solutions was purified using a laboratory-grade RO-ultrapure water system (resistivity >18.3 MΩ cm). Seawater was collected from the coastal waters near Kaohsiung, Taiwan. The concentration of Cl^- was 19,000 mg/L, and the pH value was 8.3. Before use, seawater was filtered through a cellulose membrane with a 0.45-μm pore size to remove suspended organic matter. The major composition of seawater is displayed in Table 1.

2.2. Batch degradation experiments

Batch experiments were conducted in 12 mL amber vials capped with Teflon-coated septa. Freshly prepared PV3A-nZVI solution was added to each vial, which contained 10 mL of TCE (10 mg/L) solution. Blank vials were prepared in the same way, except PV3A-nZVI was not added. All vials were placed in a shaker at room temperature (25 ± 2°C) and continuously shaken. To investigate the effect of the TCE concentration, the TCE concentration was set to values

Table 1
Major composition of seawater

Composition	Concentration (mg/L)
Chloride (Cl^-)	19,000
Bromide (Br^-)	64
Sodium (Na^+)	10,380
Magnesium (Mg^{2+})	1,258
Calcium (Ca^{2+})	420
Potassium (K^+)	372
Total dissolved solids (TDS)	36

ranging from 5 to 40 g/L. To investigate the effect of pH, the initial pH was adjusted using H_2SO_4 or NaOH. To evaluate the effect of the sample matrix, different amounts of seawater were added to the reaction vials. Oxidation–reduction potential (WTW GmbH Co., Germany) and a pH meter (SUNTEX SP-701, Taiwan) were used for monitoring redox potential and pH changes during batch experiments. A headspace analysis of TCE concentrations was performed using an Agilent 5890 gas chromatograph equipped with a DB-624 capillary column and a flame ionization detector. The chromatography conditions were as follows: the column oven was initially maintained at 50˚C for 8 min, and the temperature was then increased to 200˚C at a heating rate of 10˚C per min. The correlation coefficient (R^2) for calibration curves should exceed 0.995, but the concentration of each standard was between ±15% of its nominal concentration. The byproducts were identified using GC–MS under the same chromatography conditions. The ion concentration was determined using an ion chromatography analyzer (Dionex DX-120). Moreover, environmental scanning electron microscopy (ESEM, FEI Quanta 200, USA) was used to obtain the morphological characteristics of the samples. X-ray diffraction (XRD, Bruker D8, Germany) was used to determine the crystallographic structure of the samples and was performed using a Cu Kα radiation source ($\lambda = 1.5406$ Å) and a scanning rate of $0.06^\circ s^{-1}$ in the incidence angle range of 15–90˚ (2θ).

3. Results and discussion

3.1. Effect of PV3A-nZVI dosage on TCE degradation

Experiments were performed using different PV3A-nZVI dosages from 1 to 20 g/L at room temperature (25 ± 2˚C) to examine their effect on TCE degradation in solutions. Fig. 1 shows the effect of the PV3A-nZVI dosage on TCE degradation. The TCE degradation efficiency ($(1 - C/C_0) \times 100\%$) increased with increases in the system PV3A-nZVI dosage (C: the residual concentration of TCE at a given reaction time and C_0: the initial TCE concentration). However, for a PV3A-nZVI dosage lower than 2 g/L, no differences were observed in the degradation efficiency. Moreover, after a reaction time of 120 min, the TCE degradation efficiency of TCE was only 45 and 46% for the system PV3A-nZVI dosages of 1 and 2 g/L, respectively. By contrast, 100% TCE degradation was achieved within 90, 30, and 15 min at PV3A-nZVI dosages of 5, 10, and 20 g/L, respectively. This phenomenon occurred because increasing system PV3A-nZVI dosages led to an increase in the number of reactive surface sites, resulting in a higher TCE degradation efficiency. The same trend has been observed in the previous studies. Joo et al. [21] reported that increasing the nZVI dosage led to an increase in the number of active sites available for the adsorption of more TCE molecules, resulting in a higher TCE removal efficiency. Shih et al. [22] and Zhang et al. [23] also demonstrated that increasing nZVI dosages led to an increase in the rate of hexachlorobenzene and 2,4,6-trinitrotoluene reduction.

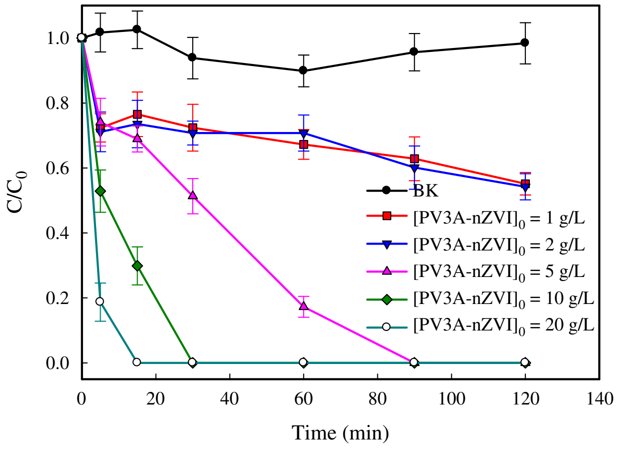

Fig. 1. Effect of PV3A-nZVI dosage on the TCE degradation in water solution ($T = 25 \pm 2$˚C, pH_0 6.8, TCE = 10 mg/L).

Fig. 2 displays the SEM images of fresh PV3A-nZVI and PV3A-nZVI after treatment with TCE. We observed that the fresh PV3A-nZVI was spherical in shape with a smooth surface. The diameter of PV3A-nZVI (approximately 2–3 μm) was larger than that of nZVI because the granulation treatment using the polymeric molecules (PV3A) could hold the nZVI particles together tightly and confine them to a granular structure. Fig. 2(b) presents the morphology of PV3A-nZVI after it reacted with TCE; the distribution of particle size was multi-model, and the micrometer-granulated PV3A-nZVI was mixed with numerous agglomerates of approximately a few tens to a few

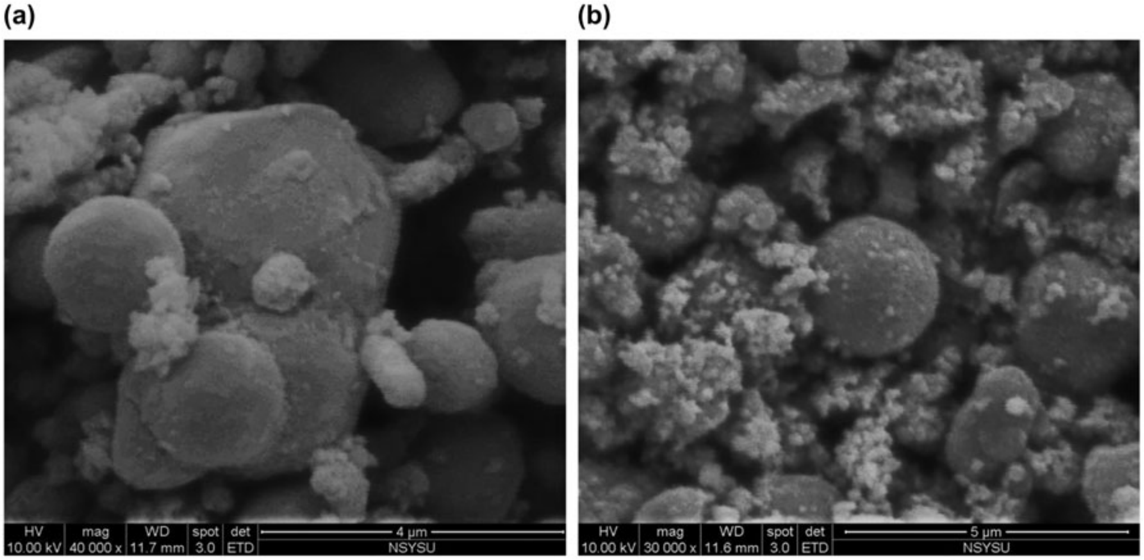

Fig. 2. SEM images of fresh PV3A-nZVI (a) and of PV3A-nZVI after treatment with TCE (b) ($T = 25 \pm 2$°C, pH_0 6.8, PV3A-nZVI = 5 mg/L; TCE = 10 mg/L; reaction time = 120 min).

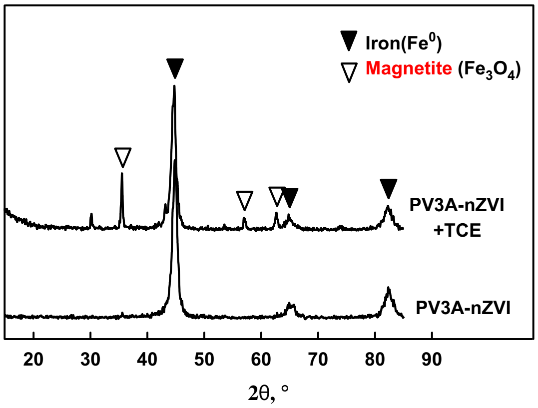

Fig. 3. XRD analysis of fresh PV3A-nZVI and of the PV3A-nZVI reaction with TCE after 120 min ($T = 25 \pm 2$°C, pH_0 6.8, PV3A-nZVI = 5 g/L, TCE = 10 mg/L).

hundreds of nanometer in size. XRD diffractograms of PV3A-nZVI (Fig. 3) suggested that small agglomerates were probably created by the precipitation of Fe_3O_4 onto the surface of PV3A-nZVI after TCE treatment. Hence, as proposed in Fig. 4, the smooth shell of the spherical micrometer pellets that were observed through SEM attacks TCE and corrodes in a very short time. However, the well-dispersed single nZVI particles inside would continuously be transported to the reactive layer containing TCE through mechanical mixing. In other words, using polymeric molecules (PV3A) to stabilize nZVI plays a crucial role in preventing the nanoparticles from forming aggregates and in prolonging the activity of nZVI.

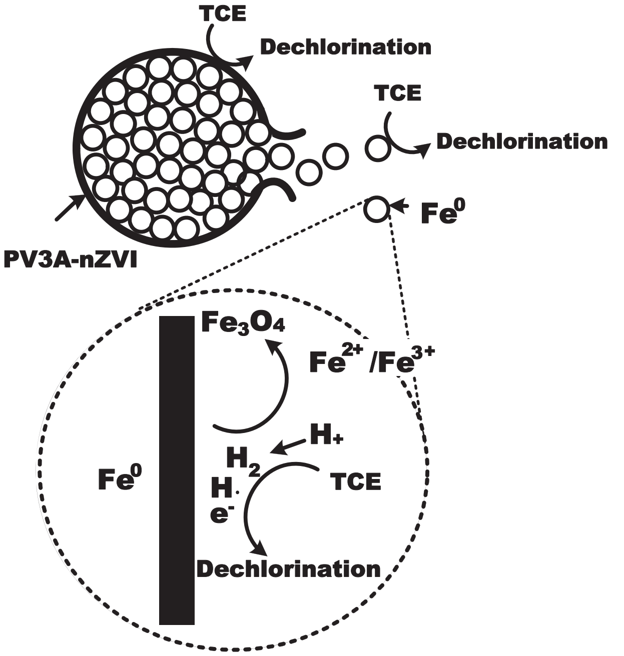

Fig. 4. A proposed mechanism for the degradation of TCE by this study.

The chloride ion (Cl^-) concentration during TCE degradation was also analyzed. Fig. 5 shows that Cl^- is released rapidly during the initial reaction step and then gradually reaches a stable state over time. The results are similar to those of the degradation experiments. Theoretically, complete mineralization of 1 mol

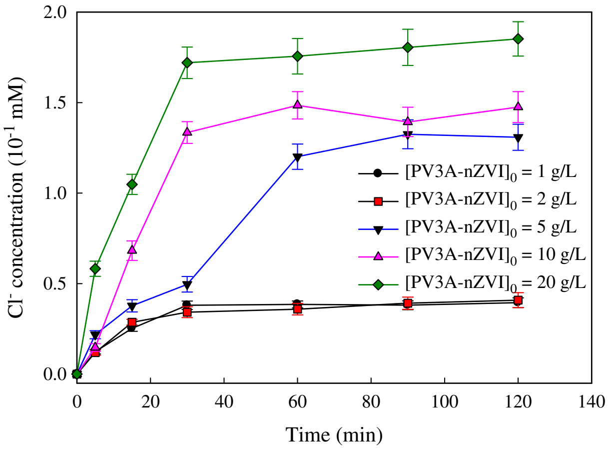

Fig. 5. Effect of different PV3A-nZVI dosages on chloride ion concentration during TCE degradation ($T = 25 \pm 2$°C, pH_0 6.8, TCE = 10 mg/L).

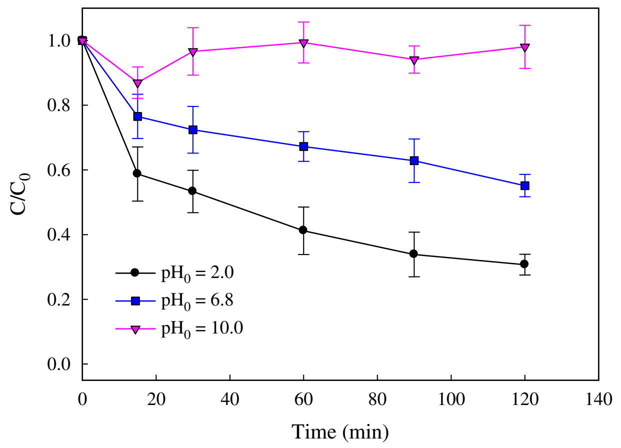

Fig. 6. Effect of initial solution pH on TCE degradation in water solution ($T = 25 \pm 2$°C, PV3A-nZVI = 1.0 g/L, TCE = 10 mg/L).

of TCE releases 3 mol of Cl^-. Cl^- released in the system (TCE = 10 mg/L; PV3A-nZVI = 20 mg/L) is 0.19 mM, and theoretically, the concentration of Cl^- released is 0.21 mM. The difference between the measured concentration and theoretical concentration of Cl^- was slight, which indicated that TCE could be completely degraded by PV3A-nZVI.

3.2. Effect of solution pH on TCE degradation

TCE degradation is strongly dependent on the solution pH. In this study, different solution pH values were tested to compare their effects on TCE degradation. As shown in Fig. 6, the effect of the initial pH on TCE degradation by PV3A-nZVI was examined at pH 2.0, 6.8, and 10.0. The TCE degradation kinetics decelerated with the increase in pH. The results obtained in this study are similar to previous findings in the literature [24,25]. As the initial pH increased from 2.0 to 6.8, the degradation efficiency decreased from 69 to 47% after a reaction time of 120 min. However, the degradation was almost terminated at the initial pH of 10.0. In general, increasing the pH promotes the formation of ferrous hydroxide. The precipitation of ferrous hydroxide on the PV3A-nZVI surface can inhibit the transport of TCE and block the reactive sites on the PV3A-nZVI surface, hence reducing the degradation reaction rate [26]. Shih et al. [22] indicated that reducing the pH causes ferrous hydroxide and other passive layers at the nZVI surface to dissolve, yielding additional reactive sites for the degradation of chlorinated organic compounds. Moreover, catalytic hydrogenation has been proposed to play a key role in dechlorination [27,28]. The fundamental steps of dehalohydrogenation by Fe-based material are depicted in Eqs. (1)–(3) [28]:

$$\mathrm{Fe} \rightarrow \mathrm{Fe}^{2+} + 2\mathrm{e}^- \tag{1}$$

$$\mathrm{Fe} + \mathrm{H}^+ + \mathrm{e}^- \rightarrow \mathrm{Fe{-}H_{ads}} \tag{2}$$

$$\mathrm{Fe{-}H_{ads}} + \mathrm{R{-}Cl} \rightarrow \mathrm{R{-}H} + \mathrm{Fe{-}Cl} \tag{3}$$

Hence, lower pH produces more Fe-based material ($Fe{-}H_{ads}$) and accelerates TCE dechlorination. Furthermore, Muftikian et al. [29] proposed that dechlorination is a consequence of direct oxidative corrosion of iron by TCE. The reaction is expressed in Eq. (4):

$$\begin{gathered}\mathrm{Fe} \rightarrow \mathrm{Fe}^{2+} + 2\mathrm{e}^-, \\ \mathrm{C_2HCl_3} + 3\mathrm{H}^+ + 6\mathrm{e}^- \rightarrow \mathrm{C_2H_4} + 3\mathrm{Cl}^-\end{gathered} \tag{4}$$

Therefore, it can be concluded that maintaining the solution pH to ensure acidic conditions can increase the effectiveness of nZVI reduction.

3.3. Effect of initial concentration on TCE degradation

Four initial TCE concentrations (5, 10, 20, and 40 mg/L) were tested to examine their effect on TCE degradation by PV3A-nZVI at room temperature. Fig. 7(a) shows the effect of the initial TCE concentration on the trend of C/C_0 during reductive dehalogenation by PV3A-nZVI. The efficiency of TCE removal decreased with the increasing initial TCE concentration. The TCE removal efficiency was nearly

80% within 30 min at an initial concentration of 5 mg/L, whereas it was only 33% at an initial concentration of 40 mg/L. Furthermore, when the initial TCE concentration was 5 mg/L, complete TCE degradation was achieved within 60 min. However, nearly 100% TCE degradation was achieved within 120 min at an initial TCE concentration of 40 mg/L under the same operating conditions. In general, increasing the initial TCE concentration results in an increase in the number of TCE molecules for adsorption on the PV3A-nZVI surface. Consequently, the total amount of degraded TCE was higher when the initial TCE concentration was higher.

Regressions of the TCE degradation data ($\ln(C_0/C)$ against time) were all close to linear ($R^2 = 0.954 - 0.981$) at the four initial TCE concentrations (Fig. 7(b)). Therefore, TCE degradation can be regarded as a pseudo-first-order kinetic reaction and written as follows:

$$\frac{-\mathrm{d}[\mathrm{TCE}]}{\mathrm{d}t} = k_{\mathrm{app}}[\mathrm{TCE}] \tag{5}$$

The obtained pseudo-first-order rate constant (k_{app}) ranged from 4.88×10^{-2} to $1.91 \times 10^{-2}\ \mathrm{min}^{-1}$ and decreased with the initial concentration (5–40 mg/L) (Fig. 7(b)). This is because an increase in TCE molecules at the PV3A-nZVI surface may produce a higher concentration of degradation intermediates. Under constant PV3A-nZVI conditions, the reactive sites on the PV3A-nZVI surface should be similar. However, the PV3A-nZVI particles have nonselective reactivity in relation to the adsorbed intermediates. Consequently, some PV3A-nZVI was used to degrade the intermediate compounds generated from TCE degradation. Thus, the apparent rate constants (k_{app}) of TCE degradation decreased with the initial concentration (5–40 mg/L).

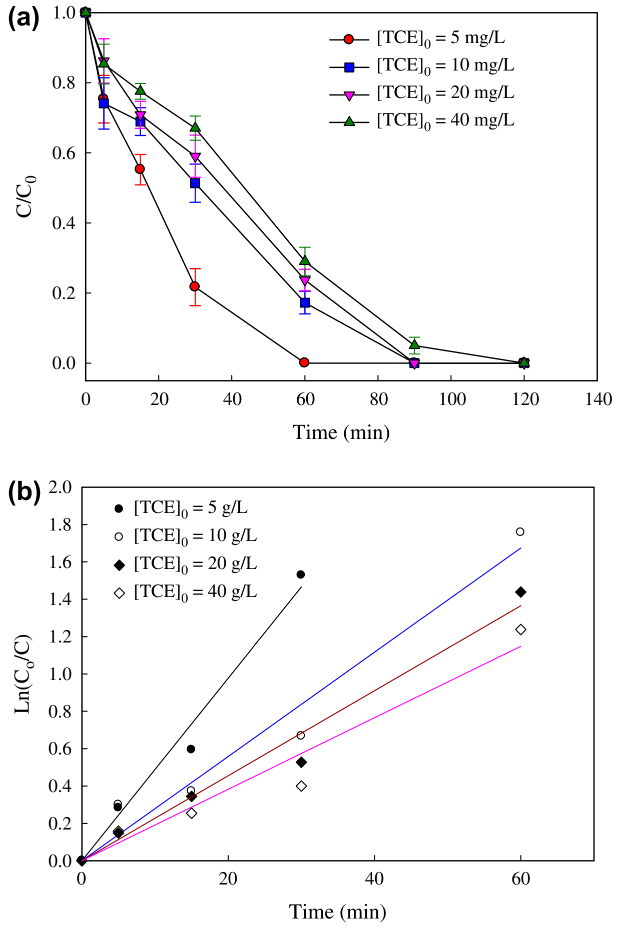

Fig. 7. (a) Effect of initial TCE concentration on TCE degradation in water solution and (b) $\ln(C_0/C)$ against time (T = 25 ± 2°C, PV3A-nZVI = 5.0 g/L, pH_0 6.8).

3.4. Effect of solution matrix on TCE degradation

To explore the effect of the solution matrix on TCE degradation, TCE degradation by PV3A-nZVI was also tested in seawater (spiked with 10 mg/L TCE and 5 g/L PV3A-nZVI in different seawater ratios). Fig. 8(a) shows a comparison of TCE degradation by PV3A-nZVI in seawater and pure water at room temperature (25 ± 2°C). The degradation efficiency of TCE decreased with the increasing seawater ratio. After 60 min, the degradation efficiency of TCE was 46, 48, 61, 72, and 83% for 100, 75, 50, 25% seawater, and pure water, respectively. The calculated degradation rate constant decreased (2.79×10^{-2} to $9.10 \times 10^{-3}\ \mathrm{min}^{-1}$) with the increase in the seawater ratio (0–100%) (Fig. 8(b)). This can be attributed to an increase in the seawater ratio producing a higher chloride concentration. Some researchers have shown that chloride ions may inhibit TCE degradation [12,25]. It has been hypothesized that the inhibitory effect is due to the passivation of reactive sites resulting from the formation of Fe–chloride complexes on the iron surface [30,31] Furthermore, the dissolved organic matter (DOM) that is originally present in seawater may affect the degradation of TCE. Lindsey and Tarr [32] reported that DOM greatly hindered the degradation of hydrophobic compounds. Zhang et al. [33] determined that introducing humic acid (HA) reduced the removal of 2,4-DCP. The inhibition of TCE removal was attributed to the competition between DOM and TCE for the surface sites on the nZVI. However, some studies have also concluded that DOM may increase the reduction of chlorinated compounds [34,35]. Wang et al. [35] indicated that the reduction of

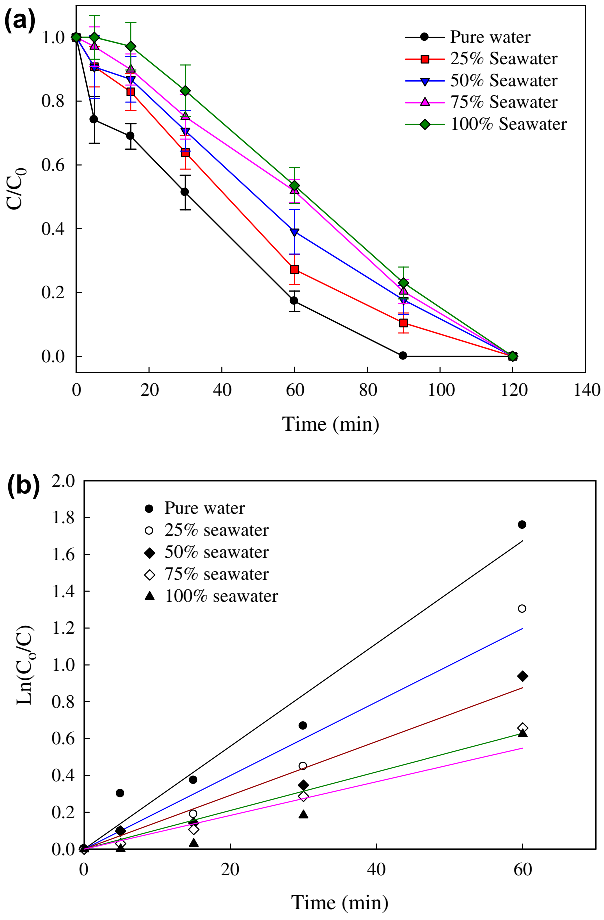

Fig. 8. (a) Effect of the sample matrix on TCE degradation and (b) ln(C_0/C) against time ($T = 25 \pm 2$°C, PV3A-nZVI = 5.0 g/L, TCE = 10 mg/L).

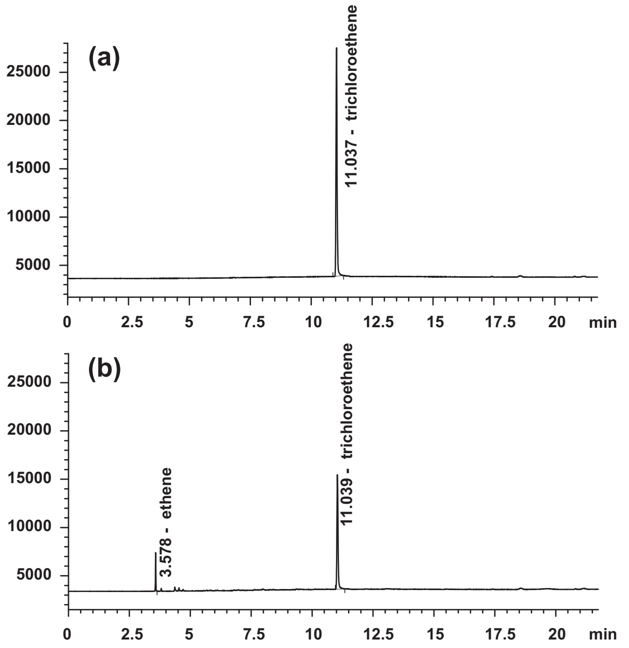

Fig. 9. GC/MS chromatogram for TCE degradation by PV3A-nZVI at (a) 0 min and (b) 15 min (TCE = 10 mg/L; PV3A-nZVI = 10 mg/L; pH_0 6.8; temperature = 25 ± 2°C).

4-chlorobiphenyl (4-ClBP) in the presence of HA increased significantly. The possible reasons are that polyphenols in the HA can reduce Fe^{3+} to Fe^{2+} and that the excavation of active surface sites by the dissolution of passive iron oxides accelerates the reduction of 4-chlorobiphenyl. Doong and Lai [34] observed the dual role of HA as both an inhibitor that competes with TCE for reactive sites and as an electron shuttle that effectively accelerates the dechlorination efficiency in the ZVI system. Therefore, studying the net effect of DOM on TCE degradation kinetics is necessary in our future work.

Some common anions such as NO_3^-, HCO_3^-, SO_4^{2-}, and CrO_4^{2-} may affect the degradation of TCE in an aqueous solution [12,36,37]. Chen et al. [12] studied the effect of various anions (NO_3^-, Cl^-, HCO_3^-, and SO_4^{2-}) at 20 mM concentrations on the degradation kinetics of TCE using stabilized zero-valent iron nanoparticles with an Na-acrylic copolymer (ac-nZVI). The calculated first-order degradation rate constants in the presence of NO_3^-, Cl^-, HCO_3^-, and SO_4^{2-} were 0.042, 0.045, 0.044, and 0.049 min^{-1}, respectively. Compared with the rate constant of 0.064 min^{-1} in the absence of these anions, common anions only slightly affect the degradation of TCE by ac-nZVI. Kaifas et al. [36] used nZVI to study TCE dechlorination in the presence of competing strong oxidants (i.e. CrO_4^{2-} and NO_3^-). The results indicated that TCE degradation and kinetic rates were inhibited in the presence of CrO_4^{2-} (20 mg/L) or NO_3^- (400 mg/L) because of the reduction of CrO_4^{2-} or NO_3^- by Fe^0, which is a corrosive process that results in the formation of a film on the Fe surface that acts as a barrier to further reactions. Surface passivation can inhibit the reduction of TCE by nZVI. Moreover, some earlier studies have indicated that adding divalent metal ions such as Ni(II), Pd(II), Cu(II), and Co(II) may enhance the dechlorination efficiency and rate of chlorinated hydrocarbons [34,35,38,39]. Wang et al. [35] studied the effect of metal ions (0.1 mM Cu^{2+}, Co^{2+}, and Ni^{2+}) on the dechlorination of 4-chlorobiphenyl by nZVI. The results indicated that adding metal ions enhanced the dechlorination efficiency of 4-ClBP. The dechlorination percentages of 4-ClBP in the presence of Cu^{2+}, Co^{2+}, and Ni^{2+} after 96 h were increased by 6.3, 2.9, and 8.5%, respectively. However, in typical seawater, the concentration of these ion species (HCO_3^-: 140 mg/L; SO_4^{2-}: 2,649 mg/L; Cr($Cr(OH)_3$, CrO_4^{2-}, $NaCrO_4^-$):

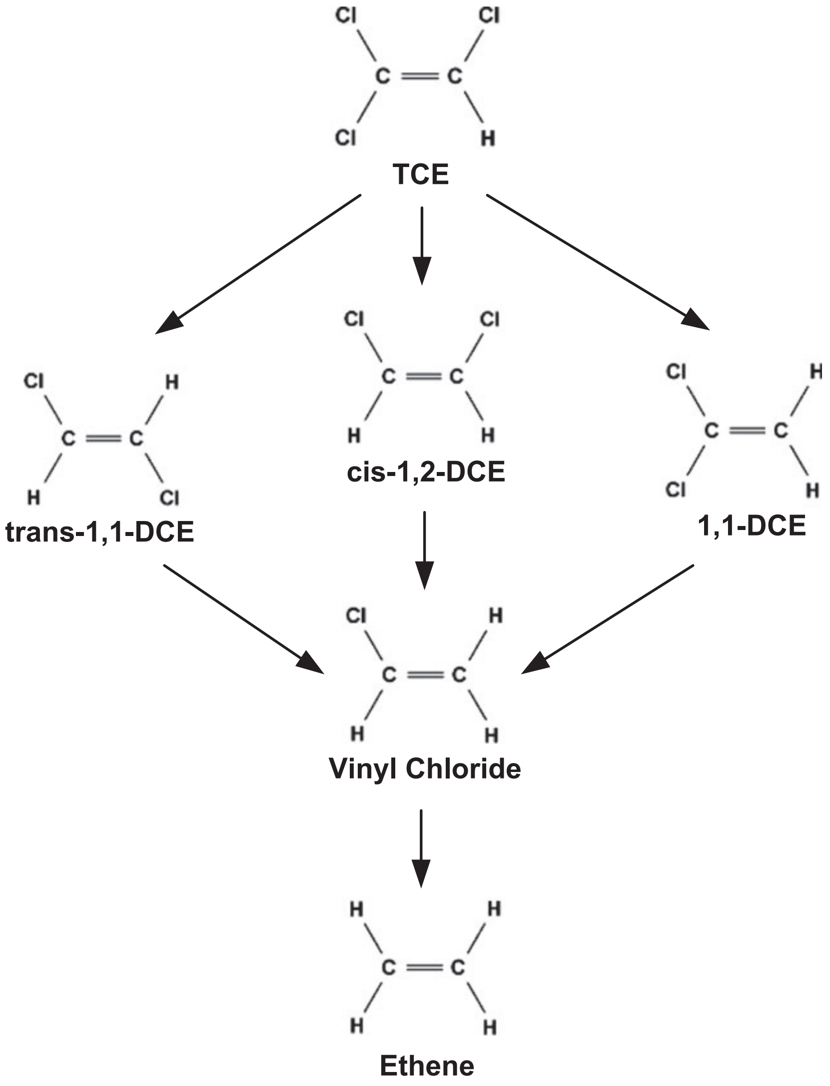

Fig. 10. Proposed dechlorination pathways of TCE degradation by PV3A-nZVI.

3×10^{-4} mg/L; Ni(II): 4.8×10^{-4} mg/L; Cu(II): 1.0×10^{-4} mg/L; and Co(II): 3.9×10^{-4} mg/L) is obviously lower than that discussed previously, except for SO_4^{2-} [40,41]. Therefore, in a real seawater matrix, the effect of these trace anions (NO_3^-, HCO_3^-, SO_4^{2-}, and $Cr_2O_4^{2-}$) and cations (Ni(II), Pd(II), Cu(II), and Co(II)) on TCE degradation could have been negligible in this study. Moreover, nearly 100% TCE removal was achieved in all tested matrices within 120 min. Hence, PV3A-nZVI is a promising technology for remediating seawater matrices that are contaminated with TCE.

3.5. TCE degradation products and pathways

To elucidate the possible mechanisms of TCE degradation, identification of the intermediate products formed during TCE degradation by PV3A-nZVI is crucial. Only a few reports have evaluated the degradation products of TCE using the photochemical method [42] and a Pd-catalytic approach [43]. Jung et al. [42] investigated the photochemical degradation of TCE through sulfite-mediated UV irradiation and found that degradation byproducts included 1,1-dichloroethylene (1,1-DCE), cis-DCE, trans-DCE, vinyl chloride (VC), chloroacetylene, ethylene, and ethane. Yuan et al. [43] indicated that the most abundant byproduct is ethane. In this study, when TCE and PV3A-nZVI concentrations were both 10 mg/L, and the solution pH_0 was 6.8, the degradation products of TCE were analyzed using GC–MS (Fig. 9). Ethene was identified; however, some chlorinated byproducts that have been reported in the previous studies such as

1,1-DCE, cis-DCE, trans-DCE, and VC were not detected after a 15-min reaction. Moreover, chloride ions are a major byproduct of TCE degradation by PV3A-nZVI. According to previous studies [42,43] and our findings, the proposed pathways for the reductive dechlorination of TCE are displayed in Fig. 10. The first step in the reductive transformation of TCE is the loss of one chlorine atom, resulting in 1,1-dichloroethylene (1,1-DCE), cis-1,2-DCE, and trans-1,2-DCE; the second step is further dechlorination to form VC. The end product is ethene. Therefore, we confirm that reductive dechlorination through the successive loss of chloride ions is the main pathway of TCE degradation by PV3A-nZVI. This finding is consistent with several studies on the reduction of chlorinated compounds by zero-valent iron [15,44,45]. However, the TCE degradation products created by PV3A-nZVI will be analyzed further in future studies.

4. Conclusions

This study thoroughly investigated the performance of PV3A-nZVI in TCE removal in an aqueous solution with different operating parameters. The experimental results showed TCE was completely degraded in pure water and seawater, and TCE degradation was a pseudo-first-order reaction. The TCE degradation efficiency increased with the increase in the system PV3A-nZVI dosage. This phenomenon occurred because increasing the system PV3A-nZVI dosage led to increases in the reactive surface sites, resulting in a higher TCE degradation efficiency.

Greater TCE removal was obtained at a low pH value, but TCE removal was suppressed at a high pH. The k_{app} values of TCE degradation decreased (4.88×10^{-2} to $1.91 \times 10^{-2}\ \mathrm{min}^{-1}$) with the increasing initial concentration (5–40 mg/L). This result can be attributed to an increase in TCE molecules at the PV3A-nZVI surface producing a higher concentration of degradation intermediates. Consequently, some PV3A-nZVI was used to degrade the intermediate compounds generated from TCE degradation. Moreover, the presence of seawater (abundant chloride) had an adverse effect on TCE removal, and a higher ratio of seawater showed higher inhibition. The investigation of TCE degradation products and pathways confirmed reductive dechlorination by the successive loss of chloride ions as the main pathway of TCE degradation by PV3A-nZVI, and ethene is the predominant byproduct. Complete degradation of 10 mg/L TCE was obtained in both pure water and seawater matrices, suggesting that the use of PV3A-nZVI is a promising approach for TCE degradation in aqueous solutions.

Acknowledgment

The authors would like to thank the Ministry of Science and Technology, Taiwan, for financially supporting this research under grants 103-2221-E-022-001-MY3 and 104-2622-E-022-001-CC2.

References

[1] P.I. Beamer, C.E. Luik, L. Abrell, S. Campos, M.E. Martínez, A.E. Sáez, Concentration of trichloroethylene in breast milk and household water from Nogales, Arizona, Environ. Sci. Technol. 46 (2012) 9055–9061.

[2] H. Clewell, P. Gentry, J. Gearhart, B. Allen, M. Andersen, Considering pharmacokinetic and mechanistic information in cancer risk assessments for environmental contaminants: Examples with vinyl chloride and trichloroethylene, Chemosphere 31 (1995) 2561–2578.

[3] U.S. EPA, Toxicity and Exposure Assessment for Children's Health. Trichloroethylene—TEACH Chemical Summary, 2007. Available from: <http://www.epa.gov/teach/chem_summ/TCE_summary.pdf>.

[4] DRC, The Domestic Market of Trichloroethylene in China, Office of Information, Beijing, 2012. Available from: <http://www.drcnet.com.cn/www/integrated/>.

[5] U.S. EPA, Tricholoethylene Health Risk Assessment: Synthesis and Characterization, External review draft. EPA/600/P-01/022A, The Office of Research and Development, Washington, DC, 2001.

[6] Z. He, G.-P. Yang, X.L. Lu, H.H. Zhang, Distributions and sea-to-air fluxes of volatile halocarbons in the East China Sea in early winter, Chemosphere 90 (2013) 747–757.

[7] M. Shao, D. Huang, D. Gu, S. Lu, C. Chang, J. Wang, Estimate of anthropogenic halocarbon emission based on measured ratio relative to CO in the Pearl River Delta region, China, Atmos. Chem. Phys. 11 (2011) 5011–5025.

[8] M.E. Alcántara-Garduño, T. Okuda, W. Nishijima, M. Okada, Ozonation of trichloroethylene in acetic acid solution with soluble and solid humic acid, J. Hazard. Mater. 160 (2008) 662–667.

[9] Y. Yokosuka, K. Oki, H. Nishikiori, Y. Tatsumi, N. Tanaka, T. Fujii, Photocatalytic degradation of trichloroethylene using N-doped TiO_2 prepared by a simple sol–gel process, Res. Chem. Intermed. 35 (2009) 43–53.

[10] T.T. Tsai, C.M. Kao, R.Y. Surampalli, C.H. Weng, S.H. Liang, Treatment of TCE-contaminated groundwater using Fenton-like oxidation activated with basic oxygen furnace slag, J. Environ. Eng. 136 (2010) 288–294.

[11] T. Li, J. Farrell, Electrochemical investigation of the rate-limiting mechanisms for trichloroethylene and carbon tetrachloride reduction at iron surfaces, Environ. Sci. Technol. 35 (2001) 60–65.

[12] M.Y. Chen, Y.F. Su, Y.H. Shih, Effect of geochemical properties on degradation of trichloroethylene by stabilized zerovalent iron nanoparticle with Na-acrylic copolymer, J. Environ. Manage. 144 (2014) 88–92.

[13] K. Choi, W. Lee, Enhanced degradation of trichloroethylene in nano-scale zero-valent iron Fenton system with Cu(II), J. Hazard. Mater. 211–212 (2012) 146–153.

[14] Y.Q. Liu, H. Choi, D. Dionysiou, G.V. Lowry, Trichloroethene hydrodechlorination in water by highly disordered monometallic nanoiron, Chem. Mater. 17(21) (2005) 5315–5322.

[15] G.V. Lowry, K.M. Johnson, Congener-specific dechlorination of dissolved PCBs by microscale and nanoscale zerovalent iron in a water/methanol solution, Environ. Sci. Technol. 38 (2004) 5208–5216.

[16] Y.P. Sun, X.Q. Li, W.X. Zhang, H.P. Wang, A method for the preparation of stable dispersion of zero-valent iron nanoparticles, Colloids Surf., A 308 (2007) 60–66.

[17] H.J. Kim, T. Phenrat, R.D. Tilton, G.V. Lowry, Fe^0 nanoparticles remain mobile in porous media after aging due to slow desorption of polymeric surface modifiers, Environ. Sci. Technol. 43 (2009) 3824–3830.

[18] K.M. Sirk, N.B. Saleh, T. Phenrat, H.J. Kim, B. Dufour, J. Ok, P.L. Golas, K. Matyjaszewski, G.V. Lowry, R.D. Tilton, Effect of adsorbed polyelectrolytes on nanoscale zero valent iron particle attachment to soil surface models, Environ. Sci. Technol. 43 (2009) 3803–3808.

[19] T. Phenrat, A. Cihan, H.J. Kim, M. Mital, T. Illangasekare, G.V. Lowry, Transport and deposition of polymer-modified Fe^0 nanoparticles in 2-D heterogeneous porous media: Effects of particle concentration, Fe^0 content, and coatings, Environ. Sci. Technol. 44 (2010) 9086–9093.

[20] Y.J. Shih, C.W. Chen, K.F. Hsia, C.D. Dong, Granulation for extended-release of nanoscale zero-valent iron exemplified by hexavalent chromium reduction in aqueous solution, Sep. Purif. Technol. 156 (2015) 1073–1081.

[21] J.C. Joo, C.H. Ahn, D.G. Jang, Y.H. Yoon, J.K. Kim, L. Campos, H. Ahn, Photocatalytic degradation of trichloroethylene in aqueous phase using nano-ZNO/Laponite composites, J. Hazard. Mater. 263 (2013) 569–574.

[22] Y.H. Shih, C.Y. Hsu, Y.F. Su, Reduction of hexachlorobenzene by nanoscale zero-valent iron: Kinetics, pH effect, and degradation mechanism, Sep. Purif. Technol. 76 (2011) 268–274.

[23] X. Zhang, Y.M. Lin, Z.L. Chen, 2,4,6 Trinitrotoluene reduction kinetics in aqueous solution using nanoscale zero-valent iron, J. Hazard. Mater. 165 (2009) 923–927.

[24] J.L. Chen, S.R. Al-Abed, J.A. Ryan, Z.B. Li, Effects of pH on dechlorination of trichloroethylene by zero-valent iron, J. Hazard. Mater. 83 (2001) 243–254.

[25] X. Zhang, X. Gu, S. Lu, Z. Miao, M. Xu, X. Fu, Z. Qiu, Q. Sui, Degradation of trichloroethylene in aqueous solution by calcium peroxide activated with ferrous ion, J. Hazard. Mater. 284 (2015) 253–260.

[26] M.M. Scherer, B.A. Balko, P.G. Tratnyek, D.L. Sparks, T. Grundl (Eds.), Mineral–Water Interfacial Reactions: Kinetics and Mechanisms, ACS Symposium No. 715, American Chemical Society, Washington, DC, 1998.

[27] Y.H. Shih, Y.C. Chen, M.Y. Chen, Y.T. Tai, C.P. Tso, Dechlorination of hexachlorobenzene by using nanoscale Fe and nanoscale Pd/Fe bimetallic particles, Colloids Surf., A 332 (2009) 84–89.

[28] Y.L. Jiao, C.C. Qiu, L.H. Huang, K.X. Wu, H.Y. Ma, S.H. Chen, L.M. Ma, D.L. Wu, Reductive dechlorination of carbon tetrachloride by zero-valent iron and related iron corrosion, Appl. Catal. B: Environ. 91 (2009) 434–440.

[29] R. Muftikian, Q. Fernando, N. Korte, A method for the rapid dechlorination of low molecular weight chlorinated hydrocarbons in water, Water Res. 29 (1995) 2434–2439.

[30] M.M. Benjamin, Water Chemistry, McGraw-Hill Company, New York, NY, 2002.

[31] M.C. Lu, Y.F. Chang, I.M. Chen, Y.Y. Huang, Effect of chloride ions on the oxidation of aniline by Fenton's reagent, J. Environ. Manage. 75 (2005) 177–182.

[32] M.E. Lindsey, M.A. Tarr, Inhibition of hydroxyl radical reaction with aromatics by dissolved natural organic matter, Environ. Sci. Technol. 34 (2000) 444–449.

[33] Z. Zhang, N. Cissoko, J. Wo, X. Xu, Factors influencing the dechlorination of 2,4-dichlorophenol by Ni–Fe nanoparticles in the presence of humic acid, J. Hazard. Mater. 165 (2009) 78–86.

[34] R.A. Doong, Y.L. Lai, Effect of metal ions and humic acid on the dechlorination of tetrachloroethylene by zerovalent iron, Chemosphere 64(3) (2006) 371–378.

[35] Y. Wang, D. Zhou, Y. Wang, X. Zhu, S. Jin, Humic acid and metal ions accelerating the dechlorination of 4-chlorobiphenyl by nanoscale zero-valent iron, J. Environ. Sci. 23(8) (2011) 1286–1292.

[36] D. Kaifas, L. Malleret, N. Kumar, W. Fétimi, M. Claeys-Bruno, M. Sergent, P. Doumenq, Assessment of potential positive effects of nZVI surface modification and concentration levels on TCE dechlorination in the presence of competing strong oxidants, using an experimental design, Sci. Total Environ. 481 (2014) 335–342.

[37] H.S. Kim, J.Y. Ahn, C. Kim, S. Lee, I. Hwang, Effect of anions and humic acid on the performance of nanoscale zero-valent iron particles coated with polyacrylic acid, Chemosphere 113 (2014) 93–100.

[38] L. Gui, R.W. Gillham, M.S. Odziemkowski, Reduction of N-nitrosodimethylamine with granular iron and nickel-enhanced iron. 1. Pathways and kinetics, Environ. Sci. Technol. 34 (2000) 3489–3494.

[39] C.J. Lin, S.L. Lo, Y.H. Liou, Dechlorination of trichloroethylene in aqueous solution by noble metal-modified iron, J. Hazard. Mater. 116 (2004) 219–228.

[40] J.F. Anthoni, The Chemical Composition of Seawater, 2006. Available from: <http://www.seafriends.org.nz/oceano/seawater.htm>.

[41] http://www.lenntech.com/composition-seawater.htm.

[42] B. Jung, H. Farzaneh, A. Khodary, A. Abdel-Wahab, Photochemical degradation of trichloroethylene by sulfite-mediated UV irradiation, J. Environ. Chem. Eng. 3 (2015) 2194–2202.

[43] S. Yuan, M. Chen, X. Mao, A.N. Alshawabkeh, Effects of reduced sulfur compounds on Pd-catalytic hydrodechlorination of trichloroethylene in groundwater by cathodic H_2 under electrochemically induced oxidizing conditions, Environ. Sci. Technol. 47(18) (2013) 10502–10509.

[44] L.J. Matheson, P.G. Tratnyek, Reductive dehalogenation of chlorinated methanes by iron metal, Environ. Sci. Technol. 28 (1994) 2045–2053.

[45] H.L. Lien, W.X. Zhang, Nanoscale iron particles for complete reduction of chlorinated ethenes, Colloids Surf., A 191 (2001) 97–105.